

## Enhanced photoelectrochemical behavior of CdS/WS<sub>2</sub> heterojunction for sensitive glutathione biosensing in human serum

Yang Zang, Xin Hu, Hui Zhou, Qin Xu, Pang Huan<sup>\*</sup>, Huaiguo Xue<sup>\*</sup>

College of Chemistry and Chemical Engineering, Yangzhou University, Yangzhou, 225002, Jiangsu, P. R. China.

<sup>\*</sup>E-mail address: [huanpangchem@hotmail.com](mailto:huanpangchem@hotmail.com), [chhgxue@yzu.edu.cn](mailto:chhgxue@yzu.edu.cn)

*Received:* 10 March 2018 / *Accepted:* 31 May 2018 / *Published:* 5 July 2018

---

This work develops an enhanced photoelectrochemical biosensor for sensitive determination of glutathione (GSH) by means of the heterojunction effect of CdS/WS<sub>2</sub>. The CdS/WS<sub>2</sub> photoanode was successfully constructed through the method of stepwise assembly, and achieved around 310% increase of photocurrent response in respect to CdS quantum dots (QDs) modified electrode due to the formation of heterostructure, which was identified by the elevation of incident-photon-to-current conversion efficiency and electron lifetime. Under illumination, with the photogenerated electrons of CdS QDs tended to WS<sub>2</sub> nanosheets and sequentially driven to ITO electrode, the corresponding photogenerated holes could continuously oxidize GSH into glutathione disulfide, leading to a remarkable photocurrent change because of the efficient charge carrier separation. Under the optimized conditions, the biosensor demonstrated excellent sensing performances with the low applied bias potential of 0 V (versus Ag/AgCl), wide linear range from 20 μM to 2.5 mM, desirable detection limit of 5.82 μM, as well as high selectivity, good stability and acceptable stability. Moreover, this biosensor was also utilized to the monitoring of GSH in human serum. These results suggested this sensing strategy has a guiding significance for the development of photoelectrochemical devices, showing great prospect in molecular diagnostics and bioanalysis.

---

**Keywords:** Photoelectrochemistry; Biosensor; Heterojunction; WS<sub>2</sub>; Glutathione

### 1. INTRODUCTION

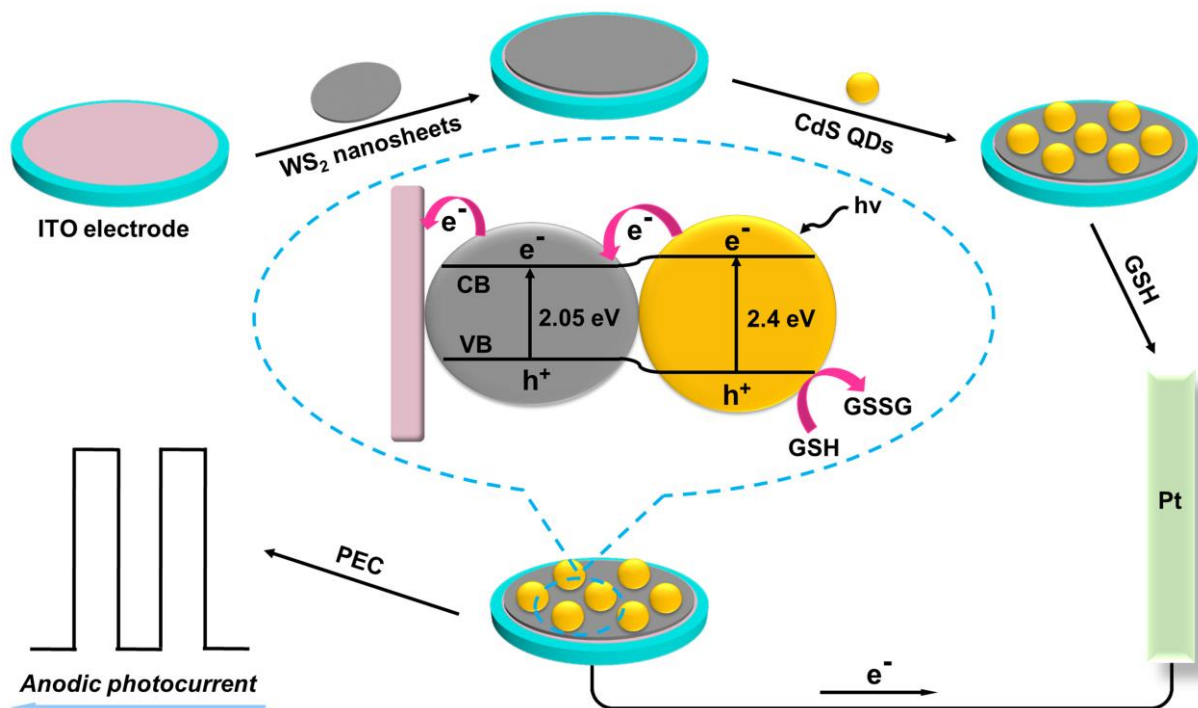
Glutathione (GSH), as the endogenous antioxidant, is a crucial thiolated tripeptide in mammalian and many prokaryotic cells, which can effectively defense against the toxins, medicines and free radicals of biological system.[1] The abnormal level of GSH is closely associated with many diseases including liver damage, leukocyte loss, rheumatoid arthritis and even cancers.[2,3] To date,

various analytical techniques have been applied for GSH assays, such as fluorescence, colorimetry, electrochemistry and surface-enhanced Raman scattering.[4-7] Nonetheless, the applications of these techniques often suffer from the limitation of low sensitivity and high cost. Therefore, exploiting a simple and sensitive testing method for GSH is still required in practice.

Photoelectrochemical (PEC) bioanalysis as a newly emerging sensing technique, in which the input signal of light and the output signal of photocurrent are completely separated, has received considerable attention owing to the high sensitivity.[8] Recently, enormous efforts have been expended to the exploitation of semiconductor quantum dots (QDs)-based PEC devices.[9-12] Among them, CdS QDs with suitable band position and gap band of 2.4 eV has been extensively employed as an important photoactive material to extend light-harvesting in visible light range, and provides a gentle environment for the determination of biomolecules.[13,14] However, its rapid recombination rate of photoinduced electron-hole pairs still exists for pure CdS QDs.[15] To alleviate this restriction, much research work has centered on the enhanced PEC property by introducing semiconductor nanomaterials with matched energy levels, which may dramatically promote the charge carriers separation.

As the analogue of graphene, 2D transition metal dichalcogenides are layered nanomaterials bounded by weak out-of-plane binding and strong in-plane interactions, have aroused growing academic interest owing to their intriguing optical, electronic and catalytic properties.[16,17] Among them, visible light-driven tungsten disulfide ( $WS_2$ ) nanosheets with a narrow band gap of around 2.05 eV, that composed of S-W-S sandwich configuration in a trigonal prismatic coordination, have exhibited promising prospect in catalyst, lithium ion batteries and field-effect transistor.[18-20] Few layers of  $WS_2$  present the large active surface and broad light absorption. Specially, in contrast with layered  $MoS_2$ ,  $WS_2$  act as a cocatalyst has the higher electrical conductivity, and is preferable for the fabrication of hybrid composites to elevate the photocatalytic activity by the integration of CdS nanomaterials. For instance, Chen et al. reported that the photocatalytic activity of CdS/ $WS_2$  heterojunction towards hydrogen evolution could be largely improved with the favorable long-time stability.[21] These results suggested  $WS_2$  has a positive function for the efficient suppression of charge carrier recombination. However, to best of our knowledge, the study on PEC sensing behavior of  $WS_2$ -supported CdS heterojunction has been less reported, which is very beneficial for the development of various bioassay methods for sensitive monitoring of analysts.

In this work, we designed an enhanced PEC sensing strategy to monitor GSH based on the excellent photoelectric property of CdS/ $WS_2$  heterojunction (Scheme 1). The PEC detection platform was constructed through the sequential assembly of  $WS_2$  nanosheets and CdS QDs. Under white light irradiation, both CdS and  $WS_2$  were excited to generate electron-hole pairs. In the presence of GSH, as the stepwise transfer of conduction band (CB) electrons of CdS QDs to ITO electrode through  $WS_2$  nanosheets, its photoinduced holes could be quickly scavenged with the oxidation of GSH to glutathione disulfide (GSSG), and the increased photocurrent response was achieved at 0 V (versus Ag/AgCl), indicating the efficient charge carrier separation of heterostructure. Thus, draw support from the superior photoelectric conversion efficiency of CdS/ $WS_2$ , the proposed biosensor exhibits the wide linear detection range and desirable selectivity.



**Scheme 1.** Schematic illustration of CdS/WS<sub>2</sub> heterojunction-enhanced PEC biosensor for sensitive detection of GSH.

## 2. EXPERIMENTAL

### 2.1. Materials and reagents

Indium tin oxide (ITO) electrode was bought from Zhuhai Kaivo Electronic Components Co. Ltd. (China). Thioglycolic acid (TGA), cadmium chloride (CdCl<sub>2</sub>), dopamine (DA), glucose, WS<sub>2</sub> and GSH were obtained from Sigma-Aldrich. Na<sub>2</sub>S·9H<sub>2</sub>O was purchased from Shanghai Lingfeng Chemical Reagent Co. Ltd. Bovine serum albumin (BSA) and ascorbic acid (AA) were available from Sangon Biological Engineering Technology & Co. Ltd. (Shanghai, China). All the chemicals were of analytical grade and used without further purification. All aqueous solutions were prepared by deionized water obtained from a Millipore water purification system (≥18 MΩ, Milli-Q, Millipore).

### 2.2. Apparatus

Scanning electron micrograph (SEM) was characterized using S-4800 field emission scanning electron microscopy (Hitachi, Japan). Transmission electron micrographs (TEM) were performed by a Tecnai 12 microscope (Philips, Netherlands). UV–vis absorption spectra were obtained using a UV-2501PC fluorescence spectrometer (Shimadzu Co. Kyoto, Japan). Photoelectrochemical measurements were performed via a home-built PEC system with white light as an accessory excitation source. Current-voltage (I-V) experiments were carried out by a CHI 660E electrochemical workstation (CH Instruments Inc., USA). Intensity-modulated photovoltage spectroscopies (IMVS) were performed on

a Zahner intensity modulated photospectrometer (Zahner, German) with a LW405 light as the excitation source. Incident-photon-to-current conversion efficiency (IPCE) data were measured in the wavelength range from 300 to 800 nm (Newport 94063, Stratford, CT, USA). Electrochemical impedance spectroscopies (EIS) were recorded using a PGSTAT30/FRA2 system (Autolab, The Netherlands) in 0.1 M Na<sub>2</sub>SO<sub>4</sub> aqueous solution containing 5 mM K<sub>4</sub>[Fe(CN)<sub>6</sub>]/K<sub>3</sub>[Fe(CN)<sub>6</sub>] (1:1) mixture as the redox probe from 0.1 Hz to 100 kHz with the applied potential of 0.180 V and a signal amplitude of 5 mV. All experiments were carried out at room temperature using a conventional three-electrode system: a modified ITO electrode (4 mm in diameter) as the working, a platinum electrode as the auxiliary, and an Ag/AgCl as the reference electrodes.

### 2.3. Synthesis of WS<sub>2</sub> nanosheets

WS<sub>2</sub> nanosheets was obtained by liquid exfoliation according to the previous work.[22] Briefly, 300 mg of bulk WS<sub>2</sub> powder was added into 100 mL of ethanol/water (the volume fraction of ethanol was 35%), and followed by ultrasonic exfoliation for 16 h. The unexfoliated aggregates could be removed from the initial dispersion by using centrifugal treatment at 3000 rpm for 20 min twice. Then, the collected supernatant was concentrated via a vacuum-rotary evaporation procedure at 70 °C. After being dissolved, the aqueous solution of WS<sub>2</sub> nanosheets was obtained and stored at 4 °C for our experiments.

### 2.4. Synthesis of CdS QDs

CdS QDs was synthesized based on the report mentioned before.[23] First, 250 μL of TGA was injected into 50 mL of 0.01 M CdCl<sub>2</sub> solution, and subsequently bubbled by highly pure N<sub>2</sub> for 30 min. In this interval, the above aqueous solution was adjusted to the favorable pH of 11 using 1.0 M NaOH. Subsequently, after 5.0 mL of 0.1 M Na<sub>2</sub>S was added, and the resulting mixture was refluxed at 110 °C for 4 h under N<sub>2</sub> atmosphere. Finally, the prepared CdS QDs was diluted by deionized water, and its storage temperature was 4 °C. Before usage, with isopropanol as a precipitant, the QDs precipitate produced by centrifugal treatment was then dissolved into the equivalent amount of water for the improvement of purity.

### 2.5. Construction and GSH detection of PEC biosensor

Before PEC biosensor was fabricated, the ITO slice was immersed in boiling 2-propanol solution containing 1.0 M NaOH for 15 min, followed by ultrasonic cleaning using 10% H<sub>2</sub>O<sub>2</sub>, acetone and deionized water. Then, 10 μL of WS<sub>2</sub> nanosheets was coated to ITO surface, and dried at ambient temperature. After CdS QDs was dropped, CdS/WS<sub>2</sub> heterostructure-based photoanode was formed via a strong surface interaction between the S layer of WS<sub>2</sub> nanosheets and Cd-rich surface of CdS QDs.[21,24] Finally, the PEC experiments of designed biosensor were investigated in 0.1 M phosphate buffer solution (PBS) of pH 7.0 with a bias potential of 0 V.

### 3. RESULT AND DISCUSSION

#### 3.1. Characterization of WS<sub>2</sub> nanosheets and CdS QDs

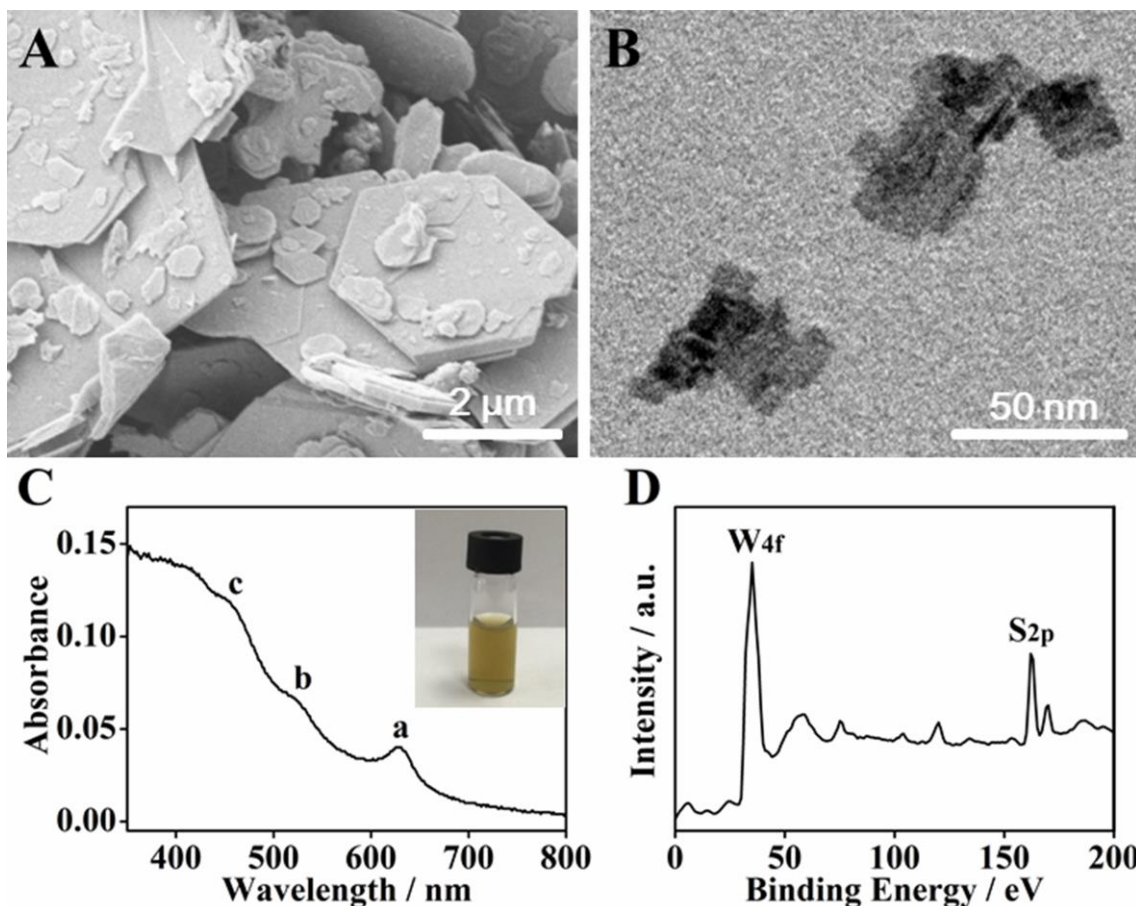


**Figure 1.** (A) SEM image of bulk WS<sub>2</sub>, (B) TEM image, (C) UV-vis and (D) XPS survey spectrum of WS<sub>2</sub> nanosheets. Inset of panel C is the photography of WS<sub>2</sub> nanosheets solution

The morphology characterization of WS<sub>2</sub> nanosheets prepared by liquid exfoliation was shown in Figure 1. Compared to the SEM image of bulk WS<sub>2</sub> (Figure 1A), the TEM image of WS<sub>2</sub> nanosheets clearly displayed well-ordered lamellar structure (Figure 1B), which was used as supporting matrixes for CdS QDs to facilitate the rapid migration of photogenerated charges via the formation of heterostructure.[25] Besides, the structural property of WS<sub>2</sub> nanosheets was investigated by UV-vis absorption spectrum. As shown in Figure 1C, two of the absorption peaks appeared at 629 nm (peak a) and 520 nm (peak b), which was related to the direct gap transitions at the K point of 2H-WS<sub>2</sub> unit cell. The weak absorption peak observed at 456 nm (peak c) was considered to be the optical transitions between the density of states in the valence band and conduction band. These finding indicated WS<sub>2</sub> nanosheets has a wider band gap than bulk WS<sub>2</sub>, and exhibited extraordinary semiconductor property.[26] In addition, the XPS spectra of WS<sub>2</sub> nanosheets was recorded in Figure 1D. As shown in Figure 1D, the peaks at 35.1 eV and 162.2 eV were the characteristic peaks of W 4f and S 2p in WS<sub>2</sub> sample. [27] Thus, these results indicated that WS<sub>2</sub> nanosheets were prepared as requested.

The TEM image of CdS QDs showed the homogeneous spherical granules with the average size of 4 nm (Figure 2A). Small size of QDs was beneficial to their photogenerated electrons transfer to WS<sub>2</sub> nanosheets. Furthermore, the yellow CdS aqueous solution was clear and transparent. To investigate the chemical components of CdS QDs by XPS, the high-resolution spectrum of Cd 3d exhibited two peaks at 404.9 eV and 411.6 eV (Figure 2B), which indicated the typical Cd 3d<sub>5/2</sub> and Cd 3d<sub>3/2</sub>, respectively. Meanwhile, Figure 2B exhibited three peaks of S 2p at 161.8 eV, C 1s at 284.9 eV and O 1s at 531.4 eV, which confirmed that CdS QDs were well-prepared for next experiments and the surfaces of QDs were stabilized by thiol ligands.[28]

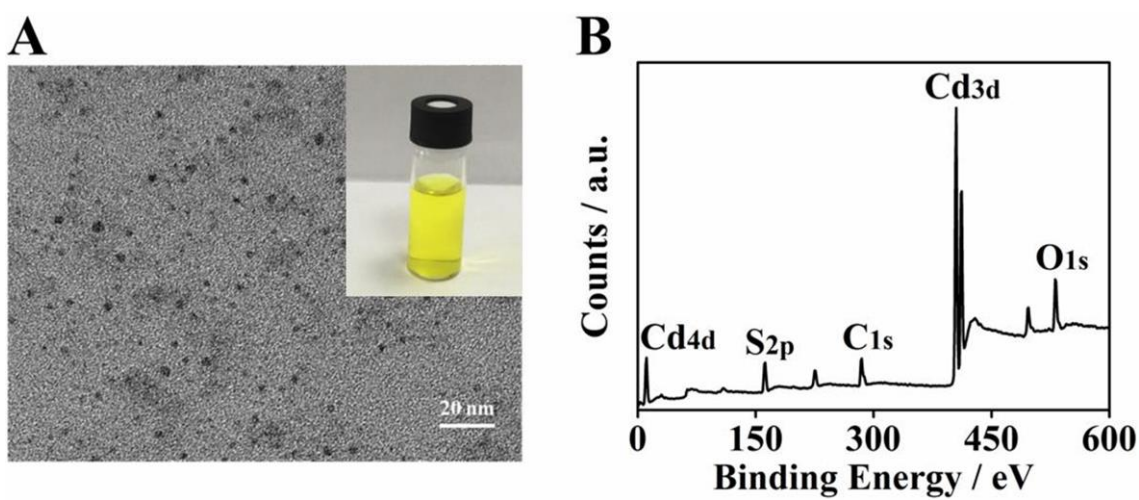


**Figure 2.** (A) TEM image and (B) XPS survey spectrum of CdS QDs. Inset of panel A is the photography of CdS QDs solution.

### 3.2. Characterization of CdS/WS<sub>2</sub> heterojunction

I-V experiments were tested to evaluate the heterojunction configuration of CdS/WS<sub>2</sub> under the potentials range from -0.1 to 1.1 V (Figure 3A). Compared with the current signal of CdS/ITO electrode (curve a), that of CdS/WS<sub>2</sub>/ITO electrode (curve b) emerged the prompt increase at applied potentials higher than 0.7 V, which involved the appearance of electrical breakdown,[29,30] indicating the high efficiently electron transfer after the introduction of WS<sub>2</sub> nanosheets. To further verify the formation of CdS/WS<sub>2</sub> heterostructure, the similar experiment phenomena were observed by IPCE. As displayed in Figure 3B, the IPCE value of CdS/WS<sub>2</sub>/ITO electrode was higher than that of CdS/ITO electrode at below 480 nm, suggesting a dramatic elevation of light harvesting capability and photoelectric conversion efficiency.[31]

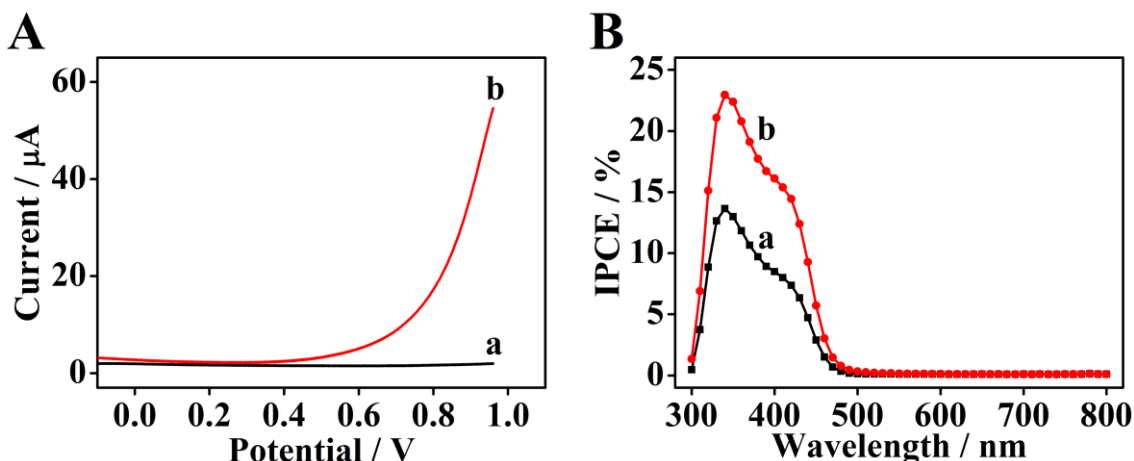


**Figure 3.** (A) I-V curves and (B) IPCE spectra of CdS (a), CdS/WS<sub>2</sub> (b) modified ITO electrodes in 0.1 M PBS of pH 7.0. Scan rate of I-V measurements: 100 mV s<sup>-1</sup>.

### 3.3. Feasibility of PEC biosensor

The stepwise fabrication of photoanode was investigated using electrochemical impedance spectroscopy (Figure 4A). Clearly, bare ITO exhibited a small interfacial charge transfer resistance ( $R_{ct}$ ) of 94.6  $\Omega$  (curve a). When WS<sub>2</sub> and CdS with poor conductivity were sequentially dropped onto the ITO surface, the  $R_{ct}$  increased to 119.4  $\Omega$  (curve b) and 187.3  $\Omega$  (curve c), respectively. These results proved that the photoanode was fabricated as expected.[32]

Moreover, to verify the feasibility of designed biosensor, the photocurrent spectra of as-prepared electrodes were investigated in different electrolytes (Figure 4B). In 0.1 M PBS of pH 7.0, a dinky photocurrent was recorded for WS<sub>2</sub>/ITO electrode (curve a), as well as a weak photocurrent for CdS/ITO electrode (curve b). And the photocurrent of CdS/WS<sub>2</sub>/ITO electrode (curve c) was higher than the sum of that of WS<sub>2</sub> and CdS modified ITO electrodes under irradiation, and the 310% increasing of photocurrent was observed for CdS/WS<sub>2</sub>/ITO electrode in contrast to CdS/ITO electrode, which indicated both CdS and WS<sub>2</sub> contributed to the enhancement of detection signal due to the effect of CdS/WS<sub>2</sub> heterostructure. When 1 mM C<sub>2</sub>H<sub>5</sub>OH was added in the above electrolyte, the photocurrent intensity of CdS/WS<sub>2</sub>/ITO electrode exhibited a negligible variation because WS<sub>2</sub>/CdS heterojunction had no strong catalytic activity toward the electron donor of alcohol in the bias potential of 0 V (curve d). However, when C<sub>2</sub>H<sub>5</sub>OH was replaced by GSH (curve e), it served as a high-efficiency electron donor to scavenge the photoinduced holes on modified electrode surface, followed by inhibiting the electron-hole pairs recombination,[33] and thus promoting the photocurrent response. These results indicated the CdS/WS<sub>2</sub>-based photoelectrode could realize the sensitive monitoring of GSH.

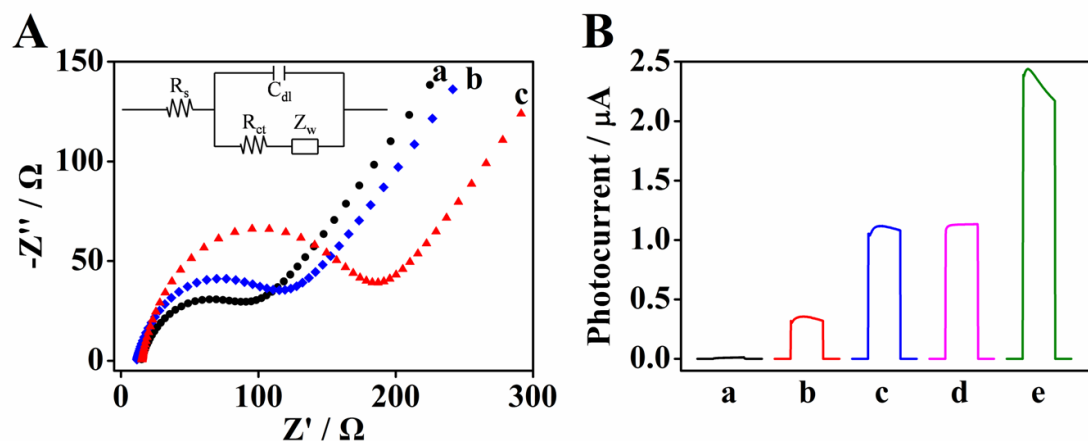


**Figure 4.** (A) Impedance spectra of bare ITO (a), WS<sub>2</sub> (b), and CdS/WS<sub>2</sub> (c). Inset: the electrical equivalent circuit applied to fit the impedance data;  $R_s$ ,  $Z_w$ ,  $R_{ct}$ , and  $C_{dl}$  represent the Ohmic resistance of the electrolyte, Warburg impedance, charge-transfer resistance, and constant phase angle element, respectively. (B) Photocurrent responses of WS<sub>2</sub> (a), CdS (b), and CdS/WS<sub>2</sub> (c) modified ITO electrodes in 0.1 M PBS of pH 7.0, CdS/WS<sub>2</sub> modified ITO electrode in 0.1 M PBS of pH 7.0 containing 1 mM C<sub>2</sub>H<sub>5</sub>OH (d), and 0.1 M PBS of pH 7.0 containing 1 mM GSH (e).

### 3.4 Optimization of detection conditions

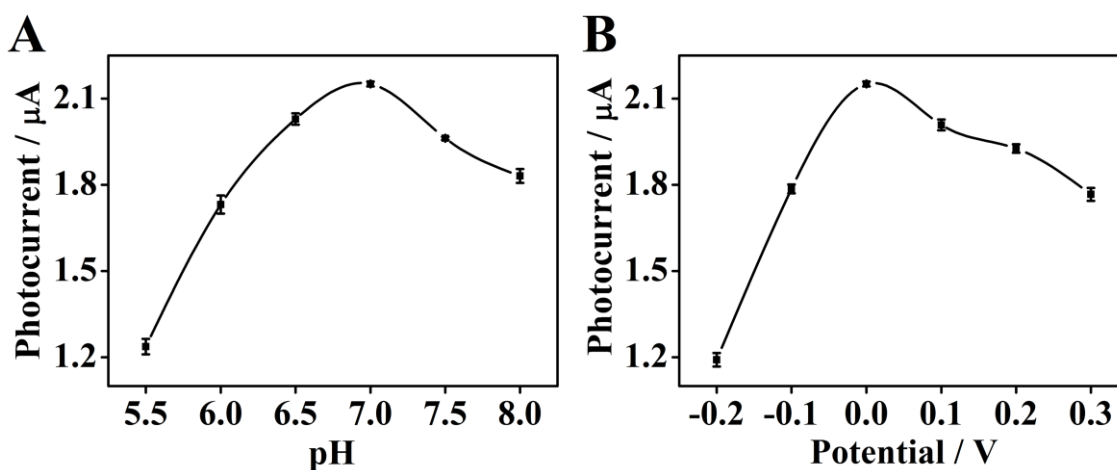


**Figure 5.** Effects of (A) pH and (B) bias potential on photocurrent responses of CdS/WS<sub>2</sub>/ITO electrode in 0.1 M PBS of pH 7.0 containing 1 mM GSH.

To optimize the detection performance of the developed biosensor, the effects of two experiment conditions, such as the pH of electrolyte and the bias potential of detection system, were studied (Figure 5A). As shown in Figure 5A, the photocurrent enhanced with the solution pH up to 7.0, and then gradually decreased when the pH value increased. Thus, pH 7.0 was chosen for the next experiments. On the other hand, the bias potential as an important parameter greatly affected the photocurrent response of biosensor (Figure 5B). Upon addition of 1 mM GSH, the photocurrent

increased sharply as an increase of bias potential and then trended toward a maximum value at 0 V. When the bias was further increased, the photocurrent decreased gradually from 0.1 to 0.3 V owing to the electrochemical oxidization of GSH at positive bias potential. And the low bias potential was beneficial to avoid the interference from other coexisted reductive species in real samples. Thus, 0 V was chosen for optimized potential.[34]

### 3.5 Analytical performances of PEC biosensor

Under optimized conditions, we accidentally found the addition of GSH could significantly enhance the photocurrent intensity in our system. Consequently, the analytical performance of the PEC biosensor for GSH assay was evaluated by time-dependent current measurement under the white light illumination (Figure 6A). As the GSH concentration increased, the intensity of photocurrent raised gradually due to the continuous oxidation of GSH by the photoinduced holes of CdS/WS<sub>2</sub>. The calibration curve of photocurrent versus GSH concentration exhibited a good linear range from 0.02 to 2.5 mM (Figure 6B). This was wider than that of self-powered PEC biosensor via CdS/RGO/ZnO nanowire heterostructure (0.05–1 mM),[35] and the fluorescence biosensor using rhodamine B-based fluorescent probe (5–80 μM).[36] The linear regression equation was  $I (\mu\text{A}) = 1.28 + 8.42 \times 10^{-4} C_{\text{GSH}}$  with a correlation coefficient of 0.998. The detection limit was calculated to be 5.82 μM (S/N = 3), which was lower than 30 μM of PEC biosensor based on porphyrin-functionalized TiO<sub>2</sub>,[37] and 8.3 μM of electrochemiluminescence sensing based on CdTe QDs with the participation of graphene oxide.[38] The more information on the comparison of different sensing methods was shown in Table 1. Apparently, the CdS/WS<sub>2</sub>/ITO photoanode with desirable PEC activity could be realized to the sensitive GSH bioanalysis.

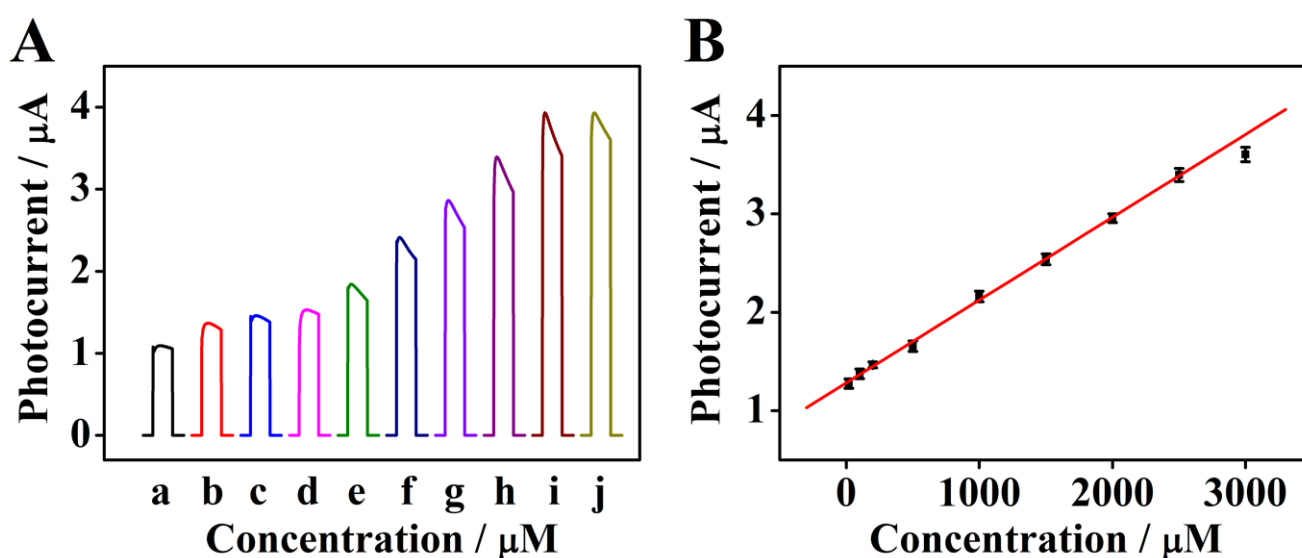


**Figure 6.** (A) Photocurrent responses of the designed biosensor at 0, 20, 100, 200, 500, 1000, 1500, 2000, 2500 and 3000 μM GSH (from a to j). (B) Calibration curve of photocurrent versus GSH concentration.

**Table 1.** Comparison of glutathione detection using various methods.

Materials	Detection methods	Linear range ( $\mu\text{M}$ )	Detection limit ( $\mu\text{M}$ )	References
Rhodamine B-based fluorescent probe	Fluorescence	5–80	0.819	[36]
Carbon QDs	Fluorescence	1–50	0.943	[39]
Eu(DPA) <sub>3</sub> @Lap-Tris-Cu <sup>2+</sup>	Fluorescence	0.5–30	0.162	[40]
GO/CdTe QDs	ECL	24–214	8.3	[38]
MnO <sub>2</sub> nanosheets	ECL	0.01–2	0.0037	[41]
IrO <sub>2</sub> -hemin-TiO <sub>2</sub>	Electrochemistry	0.01–10	0.01	[2]
Carbon microfiber	Electrochemistry	5–65	0.5	[6]
Graphene-CdS	PEC	10–1500	3	[34]
CdS/reduced graphene oxide/ZnO	PEC	50–1000	10	[35]
FeTPPS-TiO <sub>2</sub>	PEC	50–2400	30	[37]
Reduced graphene layer/ZnO nanorods	PEC	10–200	2.17	[42]
Au NPs@ZnO nanorods	PEC	20–1000	3.29	[43]
Nitrogen doped graphene QDs/BiOBr	PEC	5–800	1.7	[44]
WS <sub>2</sub> /CdS	PEC	20–2500	5.82	This work

### 3.6. Selectivity, reproducibility, and stability

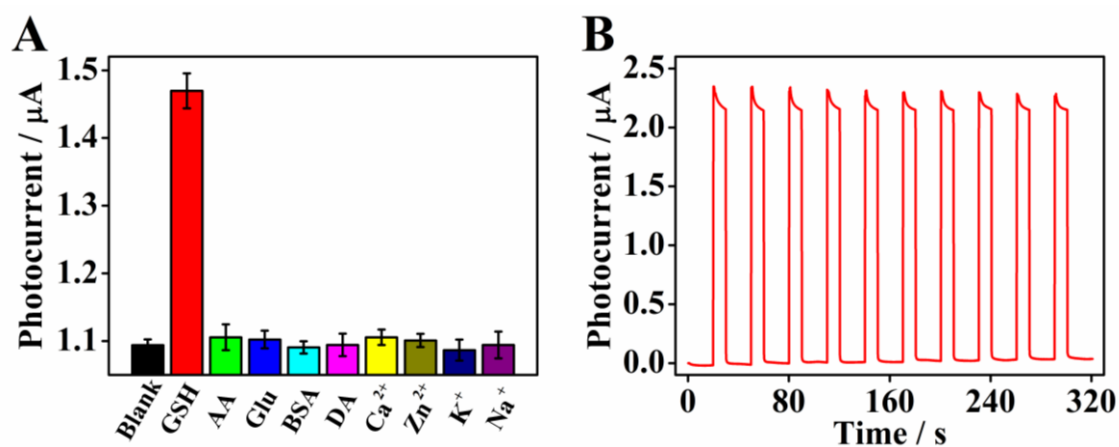


**Figure 7.** (A) Photocurrent of the biosensor in 0.1 M PBS of pH 7.0 containing 0  $\mu\text{M}$  GSH, 200  $\mu\text{M}$  GSH and some interferent species (AA, Glu, BSA, DA, Ca<sup>2+</sup>, Zn<sup>2+</sup>, K<sup>+</sup>, and Na<sup>+</sup>) at 0 V. (B) Time-based photocurrent response of CdS/WS<sub>2</sub> modified ITO electrode in 0.1 M PBS of pH 7.0 containing 1 mM GSH.

In order to test the practicality of our biosensor, the influence of several biomolecules and metal ions on the photocurrent signal was discussed to validate the selectivity of GSH assay[41]. As shown in Figure 7A, compared to the photocurrent intensity of biosensor toward 200  $\mu\text{M}$  GSH, the slight photocurrent response was observed when 200  $\mu\text{M}$  ascorbic acid, glucose, bovine serum albumin, dopamine,  $\text{Ca}^{2+}$ ,  $\text{Zn}^{2+}$ ,  $\text{K}^+$  and  $\text{Na}^+$  was added into the blank electrolyte, respectively. These results suggested that the added interfering substances had a little influence on the determination of GSH, which was ascribed to the lower bias potential of 0 V that effectively minimized the interference from other reducing substances.[43]

Besides, the stability of biosensor was also evaluated in Figure 7B. As the light was repeatedly turned on and off, the photocurrent intensity was stable and unchanged over time, which displayed the excellent detection stability. The relative standard deviation (RSD) of photocurrent toward 1mM GSH was 4.6% using five independent electrodes, giving satisfactory precision and fabrication reproducibility.[45] Moreover, the constructed photoelectrode was stored in dark place at 4  $^{\circ}\text{C}$  when not in use, and its long-time stability was also verified. After two weeks, the photocurrent did not change obviously compared with the initial photocurrent response, indicating that the structural stability of this photoanode has great practical potential for bioassays.

### 3.7 Determination of GSH in human serum

To further explore the potential application of our sensing approach, the biosensor was investigated by quantifying the GSH level in the human serum.[40] Prior to the measurements, the fresh human serum samples were appropriately diluted into the calibration range of this assay with 0.1 M PBS of pH 7.0. As shown in Table 2, the original concentration of the diluted GSH was determined as 24.57  $\mu\text{M}$ . When spiked with 50, 100, 500 and 1500  $\mu\text{M}$  GSH, the average of recoveries ranged from 95.1% to 102.6% for three PEC measurements, and the corresponding RSD was less than 5.6%, which demonstrated good accuracy and acceptable precision for monitoring clinical human serum samples.[46]

**Table 2.** GSH detection in human serum using the designed PEC biosensor.

Sample	Found in sample ( $\mu\text{M}$ )	Added ( $\mu\text{M}$ )	Total found ( $\mu\text{M}$ ) <sup>a</sup>	Recovery (%)
human serum	24.57	50	72.36 $\pm$ 4.5	95.6
		100	127.19 $\pm$ 4.7	102.6
		500	499.91 $\pm$ 3.9	95.1
		1500	1475.78 $\pm$ 4.2	96.7

<sup>a</sup> Mean of three photoelectrochemical measurements  $\pm$  standard deviation.

#### 4. CONCLUSION

In summary, an enhanced PEC biosensor for selective GSH detection was first developed based on the highly efficient heterostructure of CdS/WS<sub>2</sub>. The heterojunction was constructed by the sequential assembly of WS<sub>2</sub> nanosheets and CdS QDs, and obtained the 310% increase of photocurrent response owing to the obvious suppression of charge carrier recombination. Under white light illumination, the GSH as a model could easily oxidized into GSSG by the direct injection of photoexcited holes on electrode surface, resulting in a significant change of photocurrent. Considering the CdS/WS<sub>2</sub> heterojunction-enhanced photoconversion efficiency, the biosensor exhibited the excellent performances including wide linear range, favorable sensitivity and desirable selectivity. Moreover, this method had been successfully utilized to monitor GSH in human serum because of its resistance to environmental interferes, and endowed an instructive function for the construction of PEC devices in molecular diagnosis and bioanalysis.

#### ACKNOWLEDGEMENTS

This work was supported by the National Natural Science Foundation of China (Grants: 21605129, 21673203, 21675140), the Natural Science Foundation of the Jiangsu Higher Education Institutions of China (Grant: 16KJB150041), Postdoctoral Science Foundation of China (Grant: 2017M621830), Jiangsu Planned Projects for Postdoctoral Research Funds (Grant: 1701187B), and the Opening Foundation of State Key Laboratory of Analytical Chemistry of Life Science of Nanjing University (Grant: SKLACLS1708).

#### References

1. W.J. Niu, R.H. Zhu, S. Cosnier, X.J. Zhang, D. Shan, *Anal. Chem.*, 87 (2015) 11150.
2. J. Tang, B. Kong, Y.C. Wang, M. Xu, Y.L. Wang, H. Wu, G.F. Zheng, *Nano Lett.*, 13 (2013) 5350.
3. Z.X. Wang, P. Han, X.X. Mao, Y.M. Yin, Y. Cao, *Sens. Actuators B: Chem.*, 23 (2017) 325.
4. L.F. Chang, X.W. He, L.X. Chen, Y.K. Zhang, *Nanoscale*, 9 (2017) 3881.
5. H.H. Xu, H.H. Deng, X.Q. Lin, Y.Y. Wu, X.L. Lin, H.P. Peng, A.L. Liu, X.H. Xia, W. Chen, *Microchim. Acta.*, 184 (2017) 3945.
6. K. Ngamchuea, C.H. Lin, C. Batchelor-McAuley, R.G. Compton, *Anal. Chem.*, 89 (2017) 3780.
7. S.C. Vijayakumar, K. Venkatakrishnan, B. Tan, *ACS Appl. Mater & Interfaces*, 9 (2017) 5077.
8. W.W. Zhao, J.J. Xu, H.Y. Chen, *Chem. Rev.*, 114 (2014) 7421.
9. G.C. Fan, X.M. Shi, J.R. Zhang, J.J. Zhu, *Anal. Chem.*, 88 (2016) 10352.
10. Y. Wang, Y.L. Zhou, L. Xu, Z.W. Han, H.S. Yin, S.Y. Ai, *Sens. Actuators B: Chem.*, 257 (2018) 237.
11. M.J. Li, Y.N. Zheng, W.B. Liang, R. Yuan, Y.Q. Chai, *ACS Appl. Mater & Interfaces*, 9 (2017) 42111.
12. H.A. Li, M.Y. Zhu, W. Chen, K. Wang, *Microchim. Acta.*, 184 (2017) 4827.
13. D.Y. Xu, P.T. Xu, Y.Z. Zhu, W.C. Peng, Y. Li, G.L. Zhang, F.B. Zhang, T.E. Mallouk, X.B. Fan, *ACS Appl. Mater & Interfaces*, 10 (2018) 2810.
14. K. Zhang, W.J. Kim, M. Ma, X.J. Shi, J.H. Park, *J. Mater. Chem. A*, 3 (2015) 4803.
15. H. Zhao, Y.M. Dong, P.P. Jiang, H.Y. Miao, G.L. Wang, J.J. Zhang, *J. Mater. Chem. A*, 3 (2015) 7375.
16. H. Jeong, H.M. Oh, A. Gokarna, H. Kim, S.J. Yun, G.H. Han, M.S. Jeong, Y.H. Lee, G. Lerondel, *Adv. Mater.*, 29 (2017) 1700308.
17. A. Ghorai, S. Bayan, N. Gogurla, A. Midya, S.K. Ray, *ACS Appl. Mater. Interfaces*, 9 (2017) 558.

18. Y.X. Yuan, R.Q. Li, Z.H. Liu, *Anal. Chem.*, 86 (2014) 3610.
19. L.W. Sun, Y.L. Ying, H.B. Huang, Z.G. Song, Y.Y. Mao, Z.P. Xu, X.S. Peng, *ACS Nano*, 8 (2014) 6304.
20. Z.Y. Qin, C. Ouyang, J. Zhang, L. Wan, S.M. Wang, C.S. Xie, D.W. Zeng, *Sens. Actuators B: Chem.*, 253 (2017) 1034.
21. J.Z. Chen, X.J. Wu, L.S. Yin, B. Li, X. Hong, Z.X. Fan, B. Chen, C. Xue, H. Zhang, *Angew. Chem. Int. Ed.*, 54 (2015) 1210.
22. K.G. Zhou, N.N. Mao, H.X. Wang, Y. Peng, H.L. Zhang, *Angew. Chem. Int. Ed.*, 50 (2011) 10839.
23. Y. Zang, J.P. Lei, Q. Hao, H.X. Ju, *ACS Appl. Mater. Interfaces*, 6 (2014) 15991.
24. M. Gopannagari, D.P. Kumar, D.A. Reddy, S. Hong, M.I. Song, T.K. Kim, *J. Catal.*, 351 (2017) 153.
25. Y.H. Sang, Z.H. Zhao, M.W. Zhao, P. Hao, Y.H. Leng, H. Liu, *Adv. Mater.*, 27 (2015) 363.
26. M. Zirak, M. Zhao, O. Moradlou, M. Samadi, N. Sarikhani, Q. Wang, H.L. Zhang, A.Z. Moshfegh, *Sol. Energ. Mat. Sol. C*, 141 (2015) 260.
27. Y.Y. Zhong, G. Zhao, F.K. Ma, Y.Z. Wu, X.P. Hao, *Appl. Catal. B: Environ.*, 166 (2016) 466.
28. Y. Zang, J.P. Lei, P.H. Ling, H.X. Ju, *Anal. Chem.*, 87 (2015) 5430.
29. Q. Hao, J.P. Lei, Q.B. Wang, Y. Zang, H.X. Ju, *J. Electroanal. Chem.*, 759 (2015) 8.
30. Y. Zang, J.P. Lei, Q. Hao, H.X. Ju, *Biosens. Bioelectron.*, 77 (2016) 557.
31. F.Q. Zhan, J. Li, W.Z. Li, Y.H. Yang, W.H. Liu, Y.M. Li, *J. Power. Sources*, 325 (2016) 591.
32. Y. Li, Y.L. Wen, L.L. Wang, W. Liang, L. Xu, S.Z. Ren, Z.Y. Zou, X.L. Zuo, C.H. Fan, Q. Huang, G. Liu, N.Q. Jia, *Biosens. Bioelectron.*, 67 (2015) 364.
33. Z.P. Li, J. Zhang, Y.X. Li, S. Zhao, P.X. Zhang, Y. Zhang, J.S. Bi, G.H. Liu, Z. Yue, *Biosens. Bioelectron.*, 99 (2018) 251.
34. X.M. Zhao, S.W. Zhou, Q.M. Shen, L.P. Jiang, J.J. Zhu, *Analyst*, 137 (2012) 3697.
35. K. Zhao, X.Q. Yan, Y.S. Gu, Z. Kang, Z.M. Bai, S.Y. Cao, Y.C. Liu, X.H. Zhang, Y. Zhang, *Small*, 12 (2016) 245.
36. X.L. Wu, H. Shu, B.J. Zhou, Y.L. Geng, X.F. Bao, J. Zhu, *Sens. Actuators B: Chem.*, 237 (2016) 431.
37. W.W. Tu, Y.T. Dong, J.P. Lei, H.X. Ju, *Anal. Chem.*, 82 (2010) 8711.
38. Y. Wang, J. Lu, L.H. Tang, H.X. Chang, J.H. Li, *Anal. Chem.*, 81 (2009) 9710.
39. J.H. Pan, Z.Y. Zheng, J.Y. Yang, Y.Y. Wu, F.S. Lu, Y.W. Chen, W.H. Gao, *Talanta*, 166 (2017) 1.
40. X. Chen, Y.R. Wang, R. Chai, Y. Xu, H.R. Li, B.Y. Liu, *ACS Appl. Mater. Interfaces*, 9 (2017) 13554.
41. W.Y. Gao, Z.Y. Liu, L.M. Qi, J.P. Lai, S.A. Kitte, G.B. Xu, *Anal. Chem.*, 88 (2016) 7654.
42. Z. Kang, Y.S. Gu, X.Q. Yan, Z.M. Bai, Y.C. Liu, S. Liu, X.H. Zhang, Z. Zhang, X.J. Zhang, Y. Zhang, *Biosens. Bioelectron.*, 64 (2015) 499.
43. Z. Kang, X.Q. Yan, Y.F. Wang, Y.G. Zhao, Z.M. Bai, Y.C. Liu, K. Zhao, S.Y. Cao, Y. Zhang, *Nano Res.*, 9 (2016) 344.
44. Y.Y. Yin, Q. Liu, D. Jiang, X.J. Du, J. Qian, H.P. Mao, K. Wang, *Carbon*, 96 (2016) 1157.
45. Z.M. Huang, Q.Y. Cai, D.C. Ding, J. Ge, Y.L. Hu, J. Yang, L. Zhang, Z.H. Li, *Sens. Actuators B: Chem.*, 242 (2017) 355.
46. Y.C. Yu, J.J. Shi, X.C. Zhao, Z.Q. Yuan, C. Lu, J. Lu, *Analyst*, 141 (2016) 3305.